https://doi.org/10.5194/egusphere-2026-2889
Preprint. Discussion started: 1 June 2026

Vertical Fluxes of Dissolved Oxygen Driven by Turbulence and Diapycnal Mixing in Patagonian Fjords

Iván Pérez-Santos[1,2,3,*], Pamela Linford[2], Luis Rozas[4], Osvaldo Artal[2,5], Elías Pinilla[6], Lauren Ross[6], Patricio Díaz[1], Marcela Rojas[7], Guido Mancilla-Gutiérrez[1], Gabriel Soto[8], Ivonne Montes[9].

[1]Centro i-mar de la Universidad de Los Lagos, Puerto Montt, Chile.
[2]Center for Oceanographic Research COPAS COASTAL, Universidad de Concepción, Chile.
[3]Centro de Investigaciones en Ecosistemas de la Patagonia (CIEP), Coyhaique, Chile.
[4]Departamento de Ingeniería Civil, Universidad de los Lagos, Puerto Montt, Chile.
[5]Geodel Laboratory, Departamento de Ingeniería en Obras Civiles, Facultad de Ingeniería y Ciencias, Universidad de La Frontera, Temuco, Chile.
[6]Civil and Environmental Engineering University of Maine, Orono, ME, USA.
[7]Universidad de Valparaíso, Valparaíso, Chile.
[8]Instituto de Fomento Pesquero (IFOP), CTPA-Putemún, Castro, Chile.
[9]Instituto de Geofísica del Perú (IGP), Lima, Perú

Correspondence to: Iván Pérez-Santos (ivan.perez@ulagos.cl), https://orcid.org/0000-0002-0184-1122

Abstract.

A global inventory of oceanic dissolved oxygen (DO) indicates that only 0.6% of the ocean's oxygen originates from the atmosphere. This makes the ocean highly sensitive to both natural and anthropogenic disturbances that can disrupt the physical and biogeochemical processes governing oceanic DO dynamics. The impact of ocean deoxygenation has accelerated globally, driven by warming and diminishing deep-water ventilation. Therefore, the primary objective of this work is to quantify, for the first time, the contribution of the dissipation of turbulent kinetic energy and the diapycnal eddy diffusivity (diapycnal mixing) to water ventilation, as evidenced by the occurrence of upward oxygen transport from deep to subsurface layers denoted as positive dissolved oxygen fluxes in the northern Patagonian fjords. A vertical microstructure profiler was used to measure, with high vertical resolution, the dissipation rate of turbulent kinetic energy and the oxygen characteristics of water at approximately 160 stations in the northern Patagonian fjords during seasonal campaigns in 2023. The results showed a range of dissipation between 10^{-9} and 10^{-4} W kg^{-1}, and diapycnal mixing values ranging from 10^{-5} to 10^{-2} m^2 s^{-1}. The highest values of both variables were recorded in the Chiloé Inner Sea, where previously reported intense mixing has been attributed to tidal energy. Regarding oxygen flux records, larger positive fluxes were reported in the surface layer (10^{-5} and 10^{-3} µmol $L^{-1}s^{-1}$). Still, significant events of positive fluxes were recorded subsurface and in the deep layers of the Puyuhuapi Fjord due to intense diapycnal mixing forced by the advection of dense ocean waters. Moreover, intense turbulence contributes to positive oxygen fluxes over more of the water column than just the surface layer, especially in the Chiloé Inner Sea, driven by the interaction between the semidiurnal tides with the complex topography of the region. Moreover, double-diffusive convection appeared to be another mechanism favoring deep-water ventilation. Our results

https://doi.org/10.5194/egusphere-2026-2889
Preprint. Discussion started: 1 June 2026

highlight the importance of incorporating turbulence measurements into fjord studies to understand sensitivity to significant oxygen variability.

1 Introduction

Hypoxic conditions and lower dissolved oxygen (DO) levels in coastal waters has expanded rapidly worldwide over the past decades, mainly due to increased anthropogenic activities. However, these conditions can also result from natural causes, of which ocean physical processes play a significant role (Conley et al., 2009; Breitburg et al., 2018). Globally, a change in ocean ventilation due to warming has been found to be one of the leading causes of DO loss (2%) over the last 50 years (Schmidtko et al., 2017). Considering more local scales, the reduction of DO can significantly higher than the global average and can differ greatly between basins, e.g., DO loss between 40-50% in the Gulf of St. Lawrence and Monterey Bay, 21% in the Southern California Bight, 22%, and 16% in the Southern Ocean (Levin 2018). Fjord ecosystems are also affected by hypoxic conditions (DO values below 2 ml L^{-1}, 30 % oxygen saturation, and/or 89 µmol L^{-1}), especially in areas with irregular topography that can act to reduce or inhibit deep-water ventilation (Jackson et al., 2021; Aksnes et al., 2023; Solas et al., 2024). In the Patagonian fjords, hypoxic conditions were first reported in 1970 by the Hudson Expedition in the subsurface layer (below 100 m depth) in Puyuhuapi Fjord and the adjacent Jacaf Channel (Linford et al., 2023 and 2024). Afterward, Silva and Vargas (2014), Schneider et al. (2014), Pérez-Santos et al. (2018), and Pinilla et al. (2020) again reported hypoxia in both areas during sporadic oceanographic cruises conducted from 1995 to 2012. Additionally, hypoxic water was observed in the Almirante Montt Gulf (51.8° S/72.8° W) in southern Patagonia (Silva and Vargas, 2014). .

The studies on hypoxic conditions and low DO waters in Patagonian fjords has allowed for the determination of which oceanographic processes contribute to variability, in particular decreases, in DO, highlighting 1) the advection of hypoxic and lower DO waters by the Equatorial Subsurface Water Mass (ESSW), 2) oxygen consumption during community respiration due to the degradation of autochthonous and allochthonous organic matter, and 3) longer residence times (Linford et al., 2024). Moreover, oxygenated subsurface water enters the Patagonian fjords from the Subantarctic region, specifically the Subantarctic Water Mass (SAAW). Additionally, surface oxygenated waters enter the fjords due to the supply of colder, fresher estuarine water from river discharge and ice melting that occurs every spring and summer. Finally, vertical mixing between the SAAW and estuarine water contributed to the origin of the Modified Subantarctic water mass (MSAAW) (Siervers and Silva, 2008; Pérez-Santos et al., 2014; Pérez-Santos et al., 2021; Linford et al., 2023, 2024). The Patagonian fjords are among the few fjord systems worldwide where water masses with both low and high DO interact. Still, the mechanisms involved in controlling this interaction and their implications for water column ventilation remain insufficiently understood, which motivates the present manuscript.

Turbulence in the ocean has been widely explored and documented since the beginning of the vertical microstructure profiler era. However, its implications for re-oxygenation and water column ventilation in Patagonian fjords have not yet been directly examined. In terms of values, the lower dissipation rate of turbulent kinetic energy (ε) was registered in the deep sea with $\varepsilon=5\times10^{-10}$ W kg^{-1}, followed by $\varepsilon=3\times10^{-9}$ and 10^{-8} W kg^{-1} in the permanent and seasonal thermocline, around

https://doi.org/10.5194/egusphere-2026-2889
Preprint. Discussion started: 1 June 2026

$\varepsilon=3\times10^{-7}$ W kg^{-1} in the mixed layer, and finally, the higher values are reported in tidal channels with $\varepsilon=5\times10^{-4}$ W kg^{-1} (Thorpe 2005). In Patagonian fjords, the first turbulence measurements were collected with a Self Contained Autonomous MicroProfiler (SCAMP), allowing the estimation of ε by fitting a theoretical Bachelor spectrum to scalar temperature or salinity values (Ruddick et al. 2000; Luketina and Imberger 2001; Steinbuck et al. 2009). The results showed a range of dissipation estimates, $\varepsilon=10^{-5}$- 10^{-3} W kg^{-1}, and of diapycnal eddy diffusivities (diapycnal mixing) between 10^{-6} and 10^{-3} m^2 s^{-1}(Pérez-Santos et al., 2014). Moreover, latter mechanical turbulence was measured with a high-resolution coastal turbulence profiler (e.g., VMP-250) which registered values of dissipation up to $\varepsilon=10^{-5}$ W kg^{-1} and diapycnal mixing values of 10^{-3} m^2 s^{-1}. These intense turbulence dissipation values were collected in the Puyuhuapi Fjord and the sill of the Jacaf channel, which favored vertical mixing and, therefore, the aggregation of zooplankton and fish (Pérez-Santos et al., 2018). Additionally, directed measurements of turbulence with a VMP-500 on the eastern side of the Magellan Strait found less intense turbulence with $\varepsilon=10^{-8}$- 10^{-7} W kg^{-1} and diapycnal mixing in the order of 10^{-3} m^2 s^{-1}, but close to the seabed, turbulence was stronger with $\varepsilon=10^{-3}$ W kg^{-1} (Lozovatsky et al., 2024). Finally, the Patagonian fjords and channels are a primary candidate for studying the implications of turbulence on oxygen fluxes and, therefore, water column ventilation as has been done in previous studies in the Baltic Sea. In fact, Holtermann et al. (2022) quantified DO fluxes in the Baltic Sea using a turbulence microstructure profiler coupled with a fast-response DO sensor. In the Baltic Sea, seasonal variability in turbulence and DO flux was observed, with the lowest values recorded in summer. Additionally, mixing processes at the edges of the study area were higher than those observed at intermediate and deep zones (Holtermann et al., 2022).

In addition to in situ observations, recent advances in high-resolution hydrodynamic modeling have enabled a more detailed characterization of circulation, stratification, and mixing processes in the northern Patagonian fjords. MOSA, an operational model, has successfully reproduced the two-layer estuarine structure and the seasonal variability of stratification, demonstrating that the interaction between river discharge, tidal forcing, and wind that regulates both the intensity and spatial distribution of vertical mixing (Ruiz et al., 2021). Regional simulations have further quantified subtidal mass and property transport through the Guafo Mouth, highlighting the role of tides in modulating exchanges between the open ocean and the inland system (Mundaca et al., 2025). In this framework, variability associated with the spring–neap tidal cycle significantly alters available kinetic energy and current structure (Artal et al., 2019), suggesting a dynamical control on mixing and ventilation processes. These studies provide the physical framework required to interpret the observed distribution of turbulence and to assess its impact on vertical dissolved oxygen fluxes.

Therefore, the main goal of this work is to quantify the contribution of the dissipation rate of turbulent kinetic energy and the diapycnal mixing to water ventilation, as evidenced by positive DO fluxes in the northern Patagonian fjords. To complete this goal, a vertical microstructure profiler was used to collect turbulence, hydrographic, and DO data with high vertical resolution (64–512 Hz) from the surface layer to 400 m depth. Additionally, a hydrodynamic model was used to understand the drivers involved in the origin of intense turbulence and, consequently, the increase in oxygen fluxes.

https://doi.org/10.5194/egusphere-2026-2889
Preprint. Discussion started: 1 June 2026

2 Data and methods

2.1 Data

The *in-situ* hydrographic and micro-scale turbulence data were obtained at 56 stations distributed along the northern Patagonian fjords, covering a distance of ~950 km from the Reloncaví Fjord to the San Rafael Lagoon (Fig. 1a, Table 1). A vertical turbulence profiler model VMP-250-RDL (Fig. 2, https://rocklandscientific.com/products/profilers/vmp-250) was used for the collection of the datasets (Fig. 1b). This instrument is equipped with high-response temperature (FP07) and water conductivity (SBE7) probes, as well as two vertical shear probes (which measure mechanical turbulence in the water). The Vertical Microstructure Profiler measured the vertical shear of horizontal velocity in two orthogonal directions ($\partial u/\partial z$ and $\partial v/\partial z$) using two shear probes installed in the nose cone of the instrument (Fig. 2b). The instrument operated in a downward profiling mode, recording data at a sampling rate of 512 Hz as it descended at an optimal free-fall speed of approximately 0.7 m s^{-1}. At least two profiles were collected at each station to ensure data reliability and to assess temporal variability (Huguenard et al., 2019). As part of the data quality control procedures, a minimum profiling speed of 0.2 m s^{-1} and minimum profile duration of 20 seconds were required for a cast to be considered valid. For the computation of the Nasmyth spectrum, the dissipation length was set to 8 seconds. The high-pass filter cutoff frequency for the shear probe data was 0.4 Hz, the low-pass filter cutoff was 30 Hz, and the anti-aliasing filter cutoff was 98 Hz. Corrections for vibrations were performed following the method described by Goodman et al. (2006). Data were excluded when the instrument's inclination angle exceeded 5% (Lueck et al., 2013), and post-processing fallowed the ATOMIX guidelines (Lueck et al., 2024).

In addition to turbulence measurements collected at 512 Hz the profiler includes additional sets of temperature and conductivity sensors (JAC-CT), chlorophyll-a, and turbidity sensors, all of which operate at a sampling rate of 64 Hz. Additionally, the VMP250-RDL has been equipped with a high-response RINKO dissolved oxygen (DO) sensor (63% response in less than 1 second in water). The profiler can be deployed to depths of up to 500 meters.

Table 1. Oceanographic campaigns carried out in northern Patagonian (PN) fjords and channels.

Expeditions (Austral seasons)	Date	# of Stations	Measurements	*Tidal Coefficient and Tidal moment
PN-Summer	March 04-19, 2023	52	Temperature, Salinity, and DO_2	90 (higher) March 19, 2023 Neap tides
		47	Turbulence	
PN-Fall	May 30-June 14, 2023	56	Temperature, Salinity, and DO_2	61(medium) June 11, 2023 Neap tides
		55	Turbulence	
PN-Winter	August 6-20, 2023	56	Temperature, Salinity, and DO_2	77 (high) August 6, 2023 Neap tides
		56	Turbulence	

*Tidal coefficient obtained during Chiloe Inner Sea turbulence measurements (E8 and E10).

https://doi.org/10.5194/egusphere-2026-2889
Preprint. Discussion started: 1 June 2026

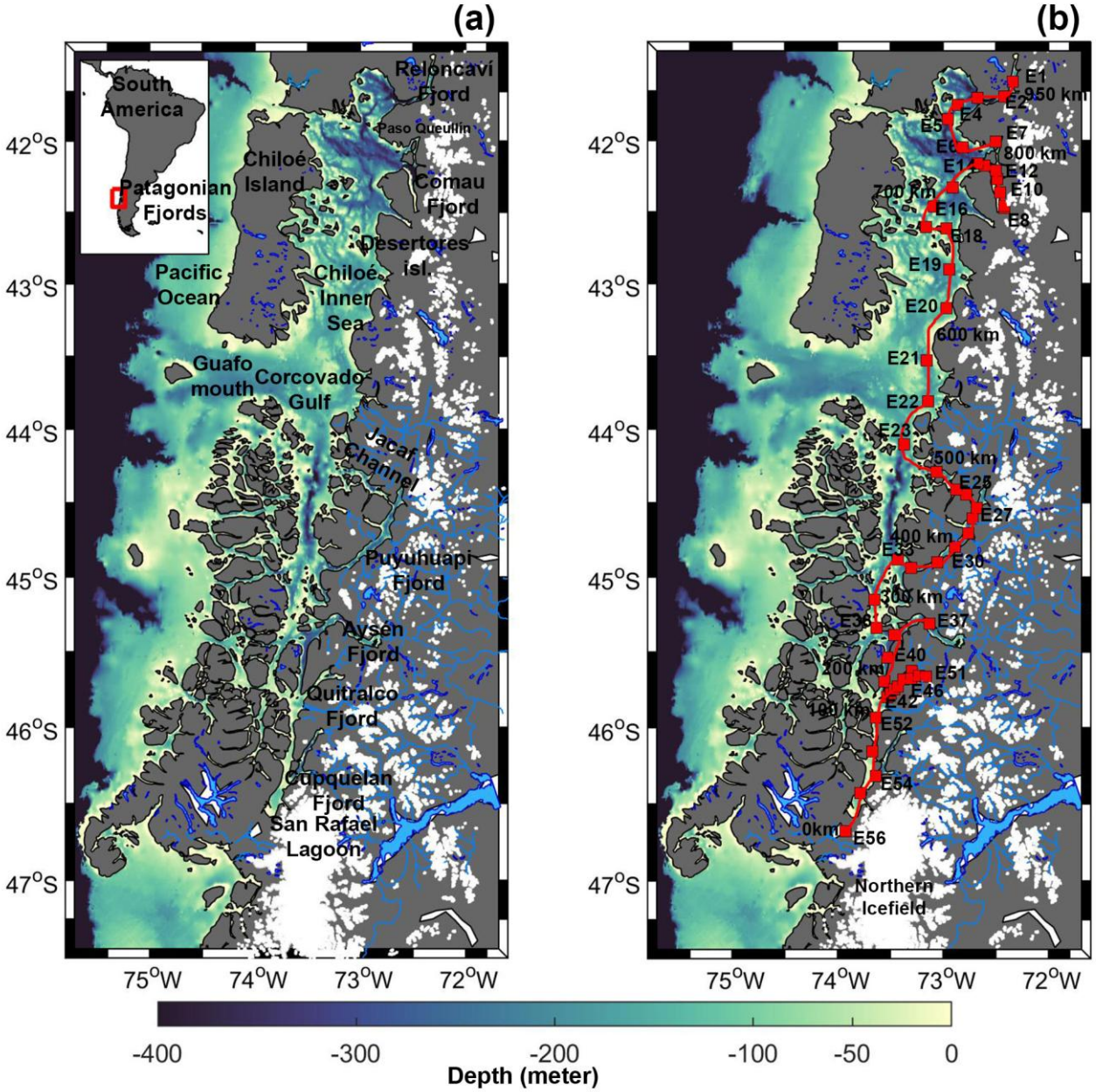

Figue. 1. (a) Map showing the fjords location in relation to South America and (b) the sampling stations carried out seasonality during 2023 in northern Patagonian fjords (all measurements described in Table 1). The rivers and lakes (blue), and snow cover (white) were added to the maps. The transect used to represent the results shown in Figures 3-6 is denoted with a continuous red line.

https://doi.org/10.5194/egusphere-2026-2889
Preprint. Discussion started: 1 June 2026

2.2 Turbulence measurements

The dissipation rate of turbulent kinetic energy (ε) obtained by the VMP-250 was derived from the vertical shear sensor records, using the following equation:

$$\varepsilon = 7.5\nu\left(\overline{\frac{\delta u}{\delta z}}\right)^2, \quad (1)$$

where, ν is the kinematic viscosity, u is the horizontal velocity, z is the vertical coordinate, and therefore $\left(\overline{\frac{\delta u}{\delta z}}\right)^2$ is the shear variance.

2.3 Dissolved oxygen fluxes calculation

We apply the methodologies proposed by Valle-Levinson (2010) and Lefor et al. (2012) to quantify the processes involved in DO variability (Equation 2).

$$\frac{\partial O}{\partial t} = \frac{\partial}{\partial z}\left(k_z \frac{\partial O}{\partial z}\right), \quad (2)$$

in which the mixing coefficient (K_z) can be calculated in terms of the diapycnal eddy diffusivity (K_ρ) and the vertical gradient of DO ($\frac{\partial O}{\partial z}$) will be measured with a JAC-CT and DO RINKO sensor. The diapycnal eddy diffusivity was referred to along the manuscript as diapycnal mixing.

The K_ρ was obtained from direct measurement of ε (Equation 1) using the VMP-250-RDL ($K_z = K_\rho$ and named in the manuscript as K_{shear}). The most frequently used formulation for K_{shear} estimation is given by:

$$K_{shear} = 2\nu\left(\frac{\varepsilon}{\nu N^2}\right)^{\frac{1}{2}} \quad (3)$$

in which ν= 1.9 × 10^{-6} m^2 s^{-1} and N is the buoyancy frequency (Osborn, 1980; Shih et al., 2005; Thorpe 2005; Cuypers et al., 2011).

When $\partial O/\partial t > 0$, oxygen is being transported upward. This process results in the release of oxygen gas from the surface layer into the atmosphere. An upward (positive) oxygen flux observed in deeper layers indicates that mechanisms are in place to ventilate the subsurface water mass, allowing oxygen to move upward from these depths. In contrast, when $\partial O/\partial t < 0$, oxygen is being transported downward. In this case, oxygen from the surface or upper layers is absorbed into the water body, rather than being released into the atmosphere or to the subsurface layers. This distinction helps clarify how oxygen dynamics can indicate whether a water body is losing, transporting, or absorbing oxygen at different depths.

https://doi.org/10.5194/egusphere-2026-2889
Preprint. Discussion started: 1 June 2026

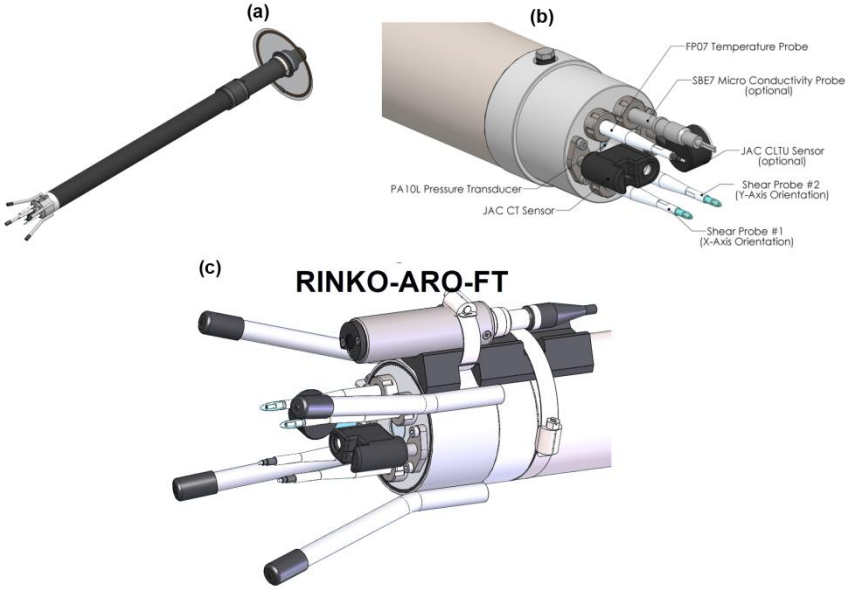

Figure 2. (a) Vertical microprofiler model VMP250-RDL with (b) two shear probes and one micro-temperature and micro-conductivity probe incorporated. (c) A fast-response DO sensor was integrated to quantify DO fluxes with the same instrument.

2.4 Numerical model

To complement field measurements and provide a regional-scale context, outputs from the South-Austral operational model MOSA (Ruiz et al., 2021) were used. MOSA consists of two components: an oceanographic component based on the Coastal and Regional Ocean Community model (CROCO, Debreu et al., 2012), and an atmospheric component based on the Weather Research and Forecasting model (WRF, Skamarock et al., 2008). CROCO has a spatial resolution of 1 km and is configured with 42 terrain-following vertical levels. The bathymetric dataset was constructed from nautical chart data from the Hydrographic and Oceanographic Service of the Chilean Navy (SHOA), complemented by data from the General Bathymetric Chart of the Oceans (GEBCO) and local multibeam datasets. WRF has a spatial resolution of 3 km and uses 32 terrain-following vertical levels. The performance of this MOSA configuration has been previously validated against hydrographic and circulation observations (Ruiz et al., 2021). Regarding tidal forcing, ten principal harmonic constituents (M_2, S_2, N_2, K_2, K_1, O_1, P_1, Q_1, M_f, and M_m) derived from the TPXO7 barotropic tidal inverse model (Egbert and Erofeeva, 2002) are currently imposed without damping.

Atmospheric forecast outputs from the WRF model (wind stress, solar radiation, longwave and shortwave heat fluxes, precipitation, and humidity) were used as surface boundary conditions for the ocean model. Similarly, oceanic boundary conditions for the water column (temperature, salinity, sea level, and currents) were interpolated from the daily 1/12° spatial resolution Mercator-Ocean product (Drévillon et al., 2008) at the open boundaries of the domain. A sponge layer 10 km wide was applied along the open boundaries to damp spurious noise and prevent the generation of artificial waves

https://doi.org/10.5194/egusphere-2026-2889
Preprint. Discussion started: 1 June 2026

caused by wave reflection at the domain edges (Penven et al., 2006). Each forecast cycle was initialized from the solution of the previous forecast to ensure dynamical continuity. Lastly, freshwater input in the model is derived from the daily climatology of 37 rivers in Chilean Patagonia, based on the FLOW hydrological model (Moreno-Meynard et al., 2024).

To highlight the high current energy within the Chiloé Inland Sea and to characterize mesoscale variability in the area, mean kinetic energy (MKE) and mean eddy kinetic energy (MEKE) were calculated. These calculations were based on the seasonally averaged simulated currents from the 2023 MOSA outputs. Summer was defined as the period from January 1 to March 30, autumn from April 1 to June 30, and winter from July 1 to September 30. MKE and MEKE were calculated as follows:

$$MKE = \frac{1}{2}(u^{-2} + v^{-2}) \quad (4)$$

$$MEKE = \frac{1}{2}(u'^{-2} + v'^{-2}). \quad (5)$$

where u and v are the zonal and meridional components of the surface current, respectively; $\bar{u}$ and $\bar{v}$ are the mean velocities; and $u' = u - \bar{u}$, $v' = v - \bar{v}$.

To explicitly characterize tidal forcing, a harmonic analysis of the simulated hourly depth-averaged currents was performed using the T_TIDE package (Pawlowicz et al., 2002). The principal semidiurnal constituent (M_2) was extracted at each grid point, obtaining the amplitudes of the zonal and meridional velocity components (A_u and A_v, respectively). From these components, the kinetic energy associated with the M_2 tidal current was estimated as:

$$KE_{M2} = 0.25(A_u^2 + A_v^2) \quad (6)$$

representing the time-averaged kinetic energy of a sinusoidal velocity signal. This metric was used to assess the spatial distribution of tidal energy and its relationship with observed turbulence.

3 Results

3.1 Hydrographic conditions and DO distribution

The vertical distribution of the water density anomaly generally showed less dense water (average of 10.5 kg m^{-3}) at the beginning of the transect (station E56 in the San Rafael Lagoon, Figure 3a-c 0 km). This station (E56) is influenced by ice melting from the San Rafael tidewater glacier (Figure 1c), which lessens density up to station E53 (e.g., Cupquelan Fjord). Conversely, the densest water was recorded in the subsurface layer (below 100 m) of the Puyuhuapi Fjord, ranging from 26−26.5 kg m^{-3} (350-550 km; stations E33-E21). The rest of the study area's density anomaly values ranged from 23 to 25 kg m^{-3} (Figures 3a-3c). In the case of DO distribution, oxygenated waters (250−320 µM) were found in the surface layer (0−50 m), and the water column was completely oxygenated in the San Rafael Lagoon (E56) and the Chiloé Inner Sea (E16−E21), as a response to the mixing processes that will be discussed in the following sections (Figures 3d-3f). Moreover,

https://doi.org/10.5194/egusphere-2026-2889
Preprint. Discussion started: 1 June 2026

we observed poorly oxygenated water (60-100 µM) in the subsurface layer of Puyuhuapi Fjord that reached hypoxic conditions. At the same time, anoxia was only observed at depth in Quitralco Fjord during all seasons (Figures 3d-3f).

When comparing the density anomaly and DO distributions highlighted through the different seasons we found: (1) densest waters were found from the Chiloé Inner Sea (E21) to the Puyuhuapi Fjord (E27−E33) during all seasons. (2) Hypoxic conditions were consistently found at water depths between 150−350 m in Puyuhuapi Fjord, but this condition was reduced in summer 2023, where hypoxia was located higher in the water column between 100−150 meters. (3) This implies that the ventilation of deep water only occurred in Summer 2023 in Puyuhuapi Fjord, which coincided with the densest waters of each season analyzed (Figures 3a and 3d). The occurrence of deep-water ventilation during the summer season raises questions about its impact on the DO flux, motivating the following sections of the manuscript.

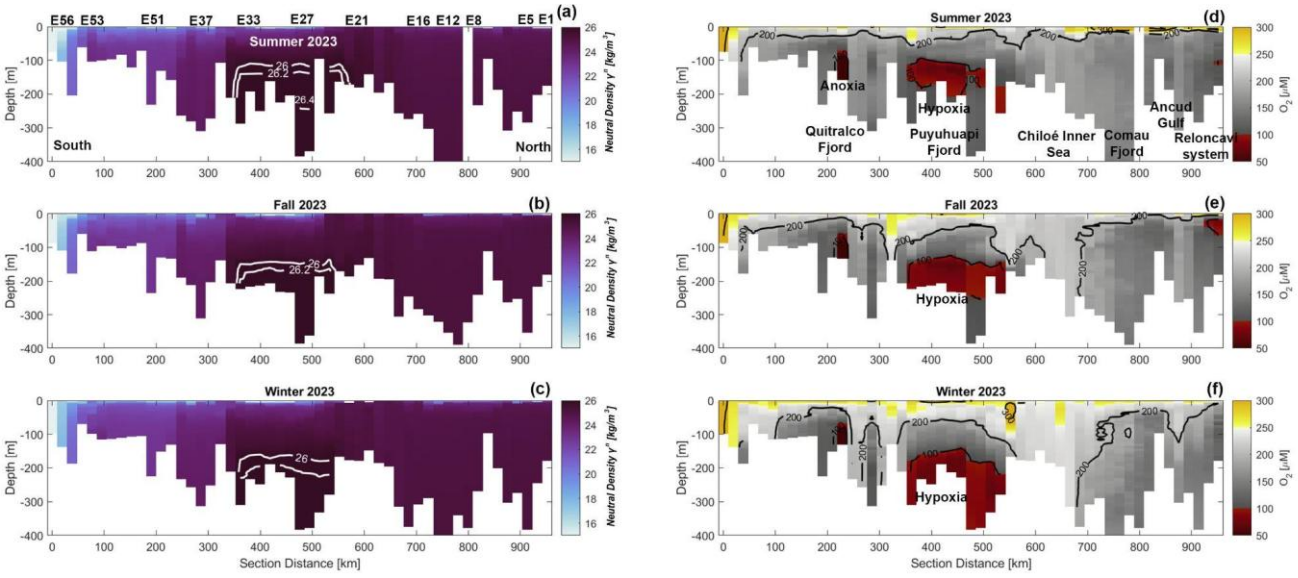

Figure 3. Seasonal vertical distribution of the (a-c) water density and (d-f) dissolved oxygen obtained from the San Rafael Lagoon (0 km, E56) to the Reloncaví Fjord (970 km, E1).

The calculation of the Brunt-Väisälä frequency to evaluate water column stratification indicated fully mixed water-column conditions in the Chiloé Inner Sea across all seasons (Figure 4), which correlated to the well-oxygenated water in this area (Figure 3d-3f). Additionally, the San Rafael Lagoon denoted thoroughly mixed conditions. At the same time, stratified waters were primarily located within the fjords, covering the top 10m of the water column, and exhibited higher values during the summer season. The oceanographic processes involved in the mixing and stratification of the water column will be examined in the discussion section.

https://doi.org/10.5194/egusphere-2026-2889
Preprint. Discussion started: 1 June 2026

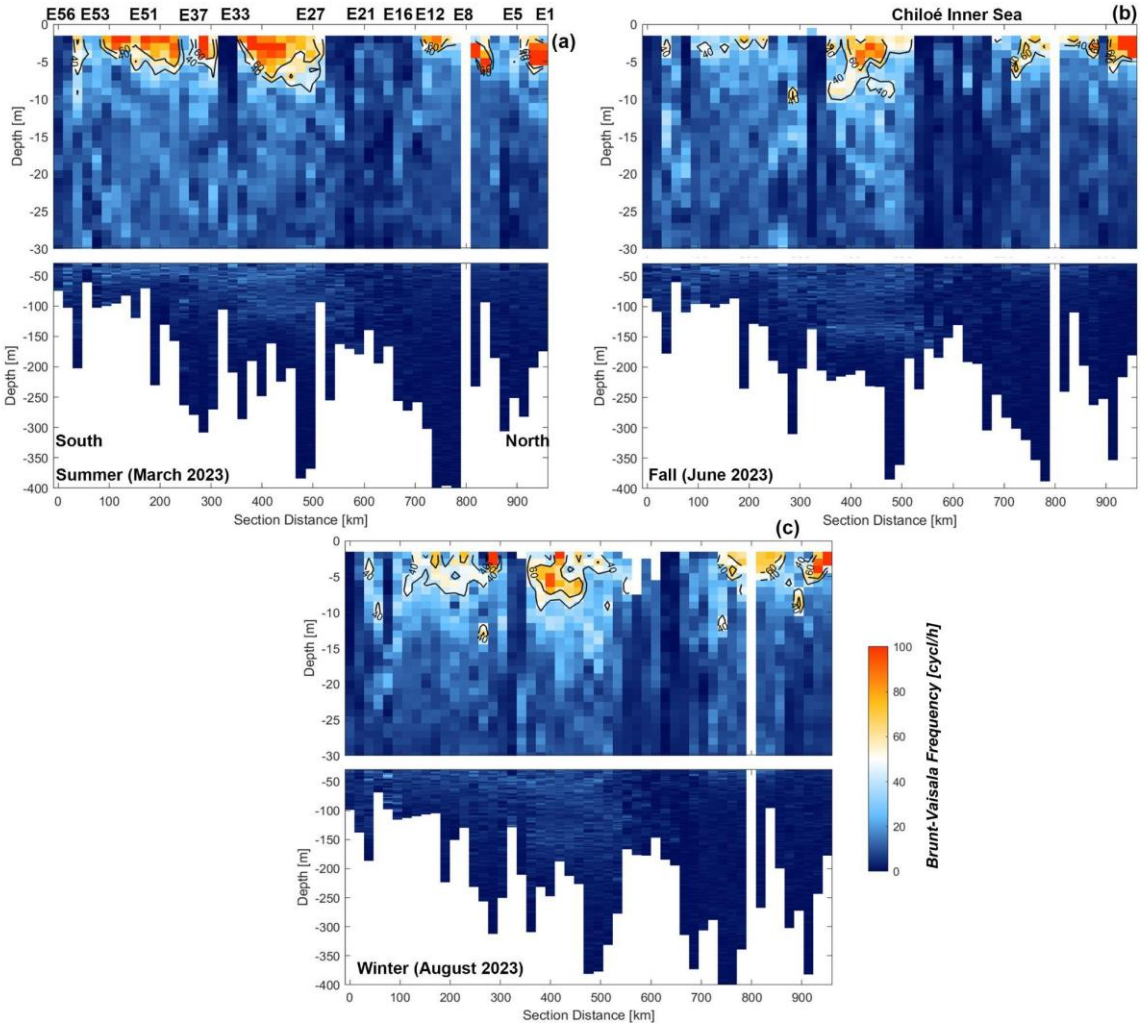

Figure 4. Seasonal records of the Brunt-Väisälä frequency along a vertical section in the northern Patagonian fjords (a) summer, (b) fall, and (c) winter during 2023.

3.2 Turbulence and mixing coefficient

As mentioned in previous sections, the Chiloé Inner Sea exhibited weak stratification and elevated DO values that extended throughout the water column (0-300 m) (Figures 3 and 4). The direct measurements of the dissipation rate of the turbulent kinetic energy (ε) revealed elevated turbulence mixing from stations E16 to E21, the area enclosed by the Corcovado Gulf and the Chiloé Inner Sea, throughout the year-round (Figure 5a-5c). In these areas, turbulent dissipation reached an absolute maximum of 4.5×10^{-4} W kg^{-1} in the surface layer during summer 2023 (Figure 5a). At station E5 (Paso Queullín) and station E53 (close to Cupquelan Fjord) high turbulent dissipation was measured during all seasons, while on average in the study area, turbulence ranged from $\varepsilon=10^{-9}$ to 10^{-5} W kg^{-1} (Figure 5).

https://doi.org/10.5194/egusphere-2026-2889
Preprint. Discussion started: 1 June 2026

The computation of the mixing coefficient calculated in terms of the diapycnal eddy diffusivity (K_{shear}) was interpreted as a competition between the turbulent mixing (∑) and the stability of the water column represented by Brunt-Väisälä frequency (N^2), according to equation 3. The K_{shear} results showed higher values in areas where turbulent dissipation was intense, with K_{shear} in the range of 10^{-3} - 10^{-2} m^2 s^{-1} (Figure 5d-5f). The absolute maximum of K_{shear} was 2.03×10^{-2} m^2 s^{-1} in the deep layer (190 m) of the Chiloé Inner Sea during winter 2023, but also in March and June 2023, K_{shear} was elevated in this area and in the subsurface layer with K_{shear} ranging between 2.2-2.8 $\times$ 10^{-2} m^2 s^{-1}. Moreover, the K_{shear} was also high outside the Chiloé Inner Sea, highlighting the subsurface and deep layer of the Reloncaví system (E1-E5), Comau Fjord (E8−E14), and Puyuhuapi Fjord (E27−E33). We will now investigate how will these results impact the DO flux in the northern Patagonian Fjords.

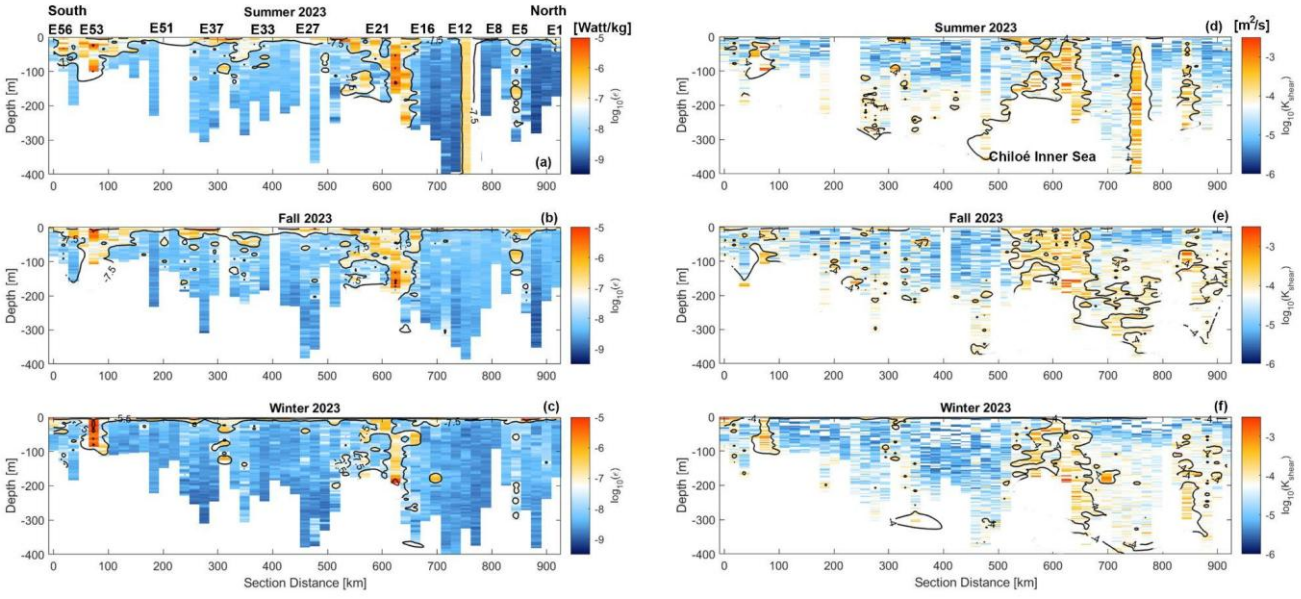

Figure 5. Seasonal vertical distribution of the (a-c) dissipation rate of turbulent kinetic energy and (d-f) diapycnal eddy diffusivity obtained from the San Rafael Lagoon (0 km, E56) to the Reloncaví Fjord (970 km, E1).

3.3 Dissolved oxygen vertical flux

As expressed in equation 2, the dissolved oxygen flux depends directly on the mixing coefficient (K_{shear}) and the vertical gradient of DO. The computation of DO flux along the 2023 seasonal campaigns (summer, fall, and winter) denoted a high number of positive events of DO flux located mainly from the subsurface layer (down 50 m) to the bottom (Figure 6a-6c), located primarily in the waters of the Reloncaví system (E1-E5), Comau Fjord (E8-E12), Chiloé Inner Sea (E16-E21), Puyuhuapi Fjord (E27-E33), and Aysén Fjord (E37). The most intense positive DO flux was obtained in the Comau Fjord (E11-E12) during summer 2023, showing values of 2×10^{-3} μMs^{-1} at 196 m, while in the Puyuhuapi Fjord (E27-E33), the deep area of positive values of DO flux expanded for about 100 km, between the 100-200 m (Figure 6a). Overall, these

https://doi.org/10.5194/egusphere-2026-2889
Preprint. Discussion started: 1 June 2026

results indicate persistent upward transport oxygen from deep to the subsurface layers, consistent with the ventilation patterns observed in several fjord systems.

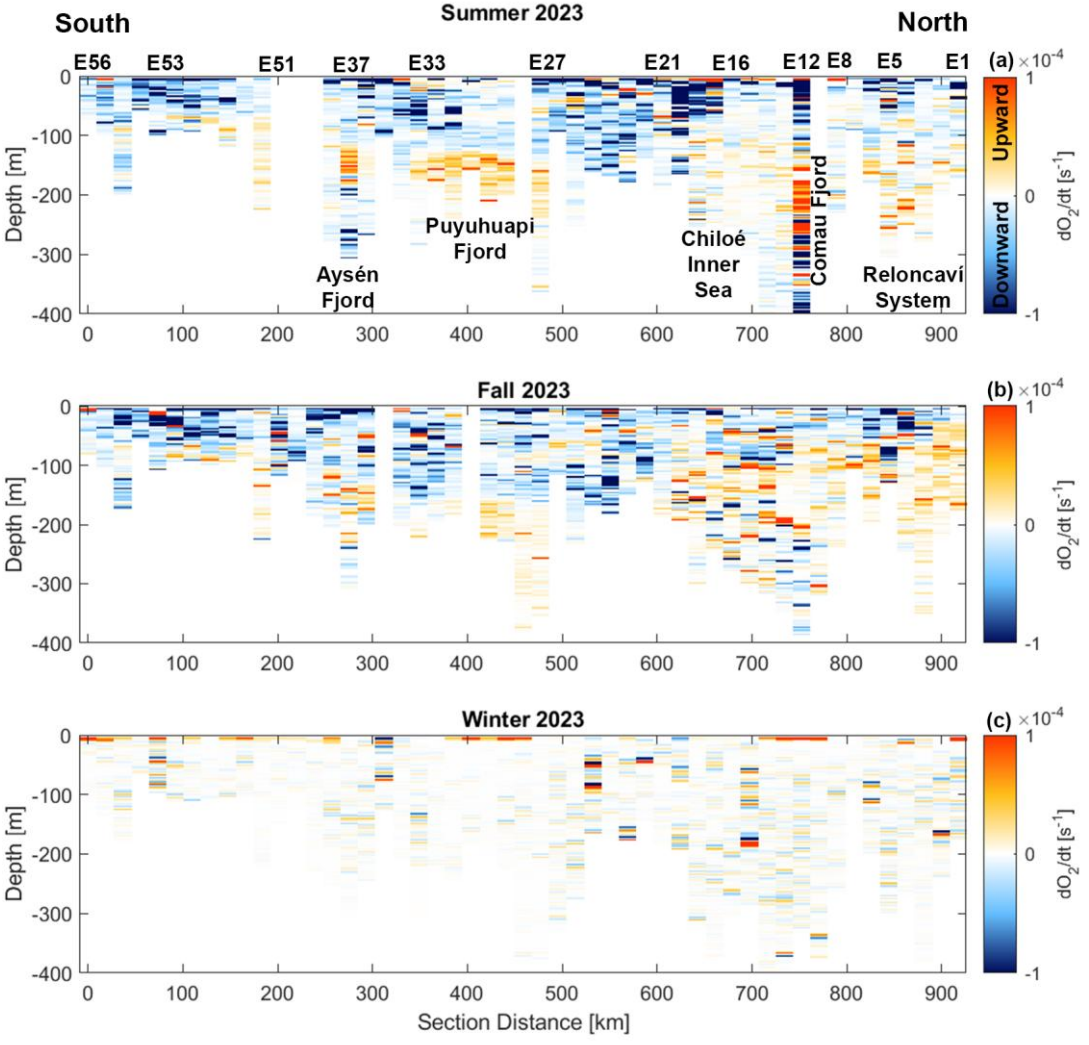

Figure 6. Seasonal vertical distribution of the (a-c) dissolved oxygen flux obtained from the San Rafael Lagoon (0 km, E56) to the Reloncaví Fjord (970 km, E1).

A histogram of frequency was applied to the DO flux calculation to quantify the seasonal differences in vertical positive DO flux occurrence in the northern Patagonian fjords. The histogram showed a significant number of records of positive DO flux in March 2023 (summer), while fewer events were observed in winter (August) 2023 (Figure 7a-7c). In the case of events detected in March 2023, a first group of records was concentrated at the surface layer (0−60 m), and a second set of events was located between 200 m and 300 m depth, which could act as confirmation of the occurrence of DO flux in the ventilation layer observed and described in the Puyuhuapi Fjord and presented in the Figure 3a and Figure 6a. We will now investigate specific DO flux profiles along the study region to confirm this.

https://doi.org/10.5194/egusphere-2026-2889
Preprint. Discussion started: 1 June 2026

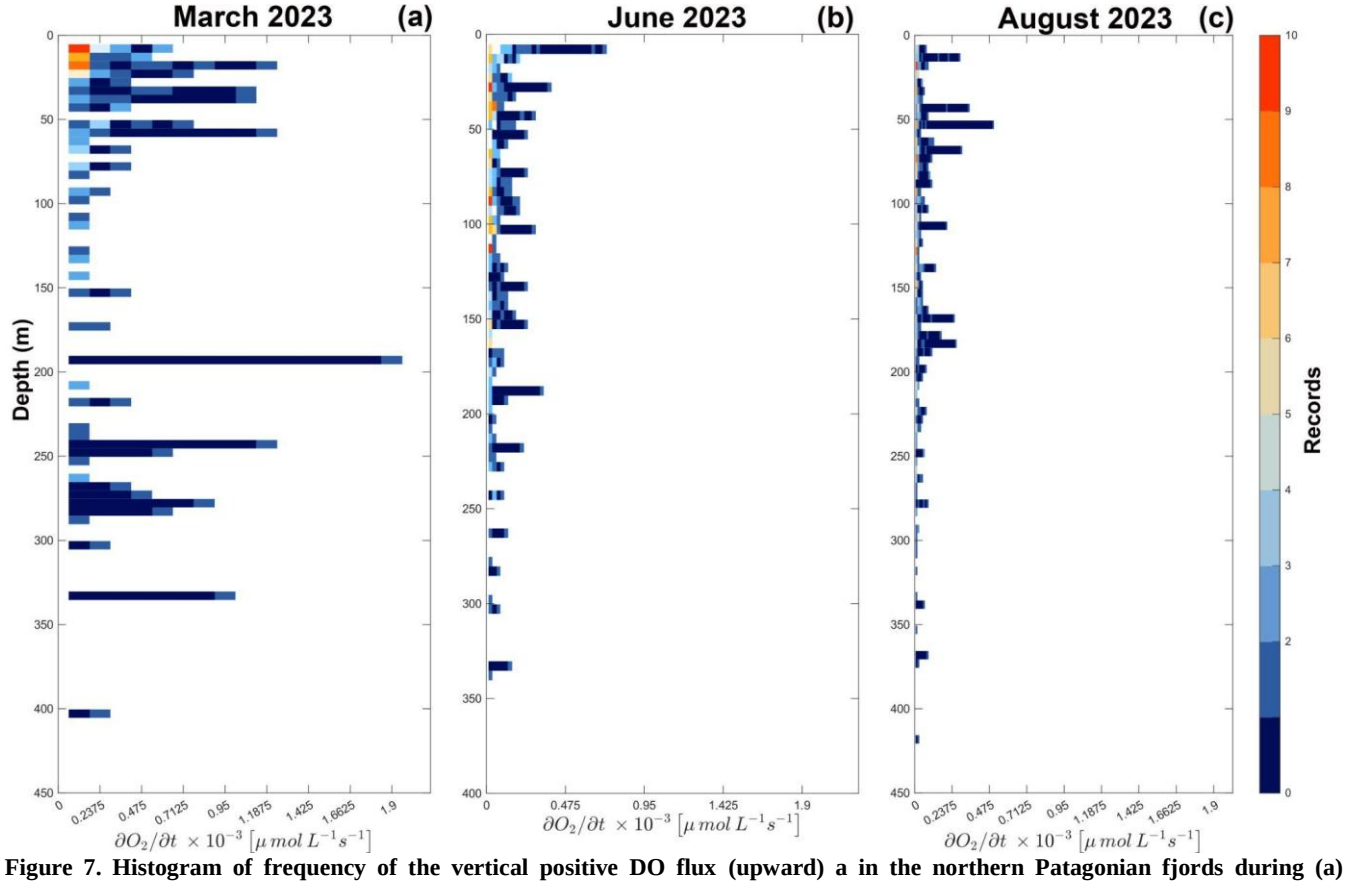

Figure 7. Histogram of frequency of the vertical positive DO flux (upward) a in the northern Patagonian fjords during (a) summer, (b) fall, and (c) winter during 2023.

A case study in Figure 8 clarified the processes involved in creating positive DO flux events. At station E8, located in the Desertores Island Passage, positive DO flux events coincided with the position where intense shear layers occurred, especially during March and June 2023, while in August 2023, turbulence was elevated homogenously over the water column, favoring positive DO flux (Figure 8a-8o). At station E19, located in the central basin of the Puyuhuapi Fjord, the intense shear layer again contributed to some positive DO flux events between the 50 m and 100 m depths. However, below these layers, turbulence decreased, and positive DO fluxes were observed (Figure 8p-8s). This relationship will be scrutinized in the discussion section. Finally, the case studies demonstrated the importance of an intense shear layer (turbulence) in generating positive DO flux events.

https://doi.org/10.5194/egusphere-2026-2889
Preprint. Discussion started: 1 June 2026

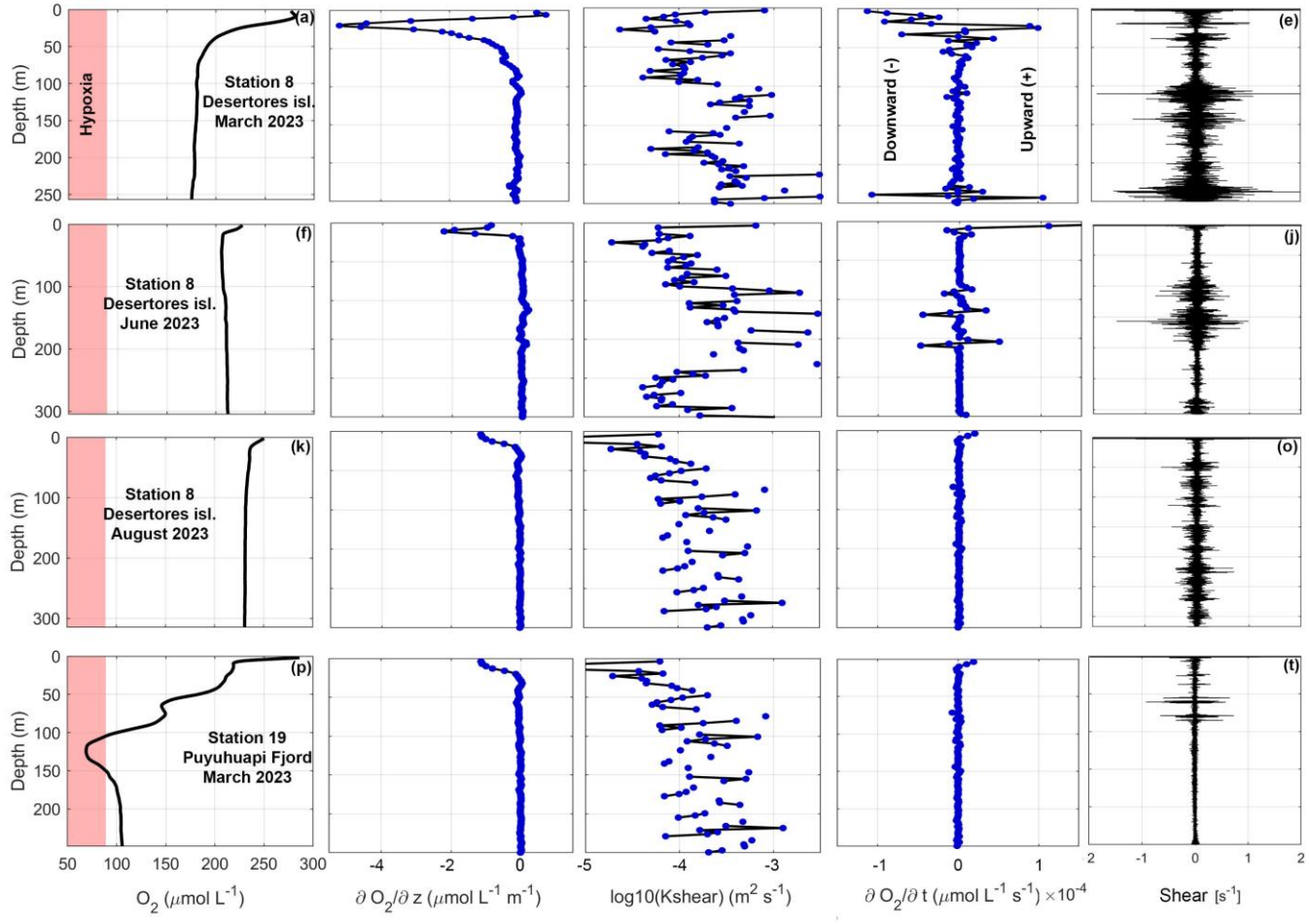

Figure 8. Examples of profiles of oxygen fluxes obtained at the intense turbulence mixing region in the Chiloé Inner Sea (E8) and in the hypoxic and ventilated region inside the Puyuhuapi Fjord (E19).

3.4 Numerical model support

To characterize the general circulation and the spatial distribution of kinetic energy in the Chiloé Inner Sea (CIS), seasonal averages of the simulated surface currents were analyzed (Fig. 9). The magnitudes of the mean kinetic energy (MKE) and mean eddy kinetic energy (MEKE) show moderate seasonal variability, particularly in the continental margin area of Chile on the eastern side of the domain (Fig. 9), which approximately corresponds to the locations of stations E5-E20. A strengthening of the surface currents is observed in this eastern region (~72° 52'W), with values around 0.25 ms^{-1} in summer (Fig. 9a) and over 0.4 ms^{-1} in winter (Fig. 9c). In the northern sector, strong currents are consistently observed across the three seasons, mainly associated with flow and circulation through the Chacao Channel. Another noteworthy feature is the enhancement of currents due to geomorphology visible during the summer near 42°45'S, with velocities of approximately 0.25 ms^{-1}. This current weakens during fall and transitions into a coastal flow that follows the Desertores

https://doi.org/10.5194/egusphere-2026-2889
Preprint. Discussion started: 1 June 2026

Passage, skirts the Desertores Islands, and continues southward along the coast. No strong currents were observed within the Comau Fjord or the Reñihué Fjord, suggesting that these current patterns following the bathymetry modulates water exchange between the fjord region and the CIS.

In turn, the spatial distribution of MKE closely follows the pattern of current magnitude, as expected. This distribution also increases from summer to winter, revealing three highly energetic regions (Figs. 9d–9f): at the northern boundary near the entrance to the Chacao Channel and the Reloncaví Sound; south of the Desertores Islands along the eastern coastal margin; and around the northern and southern sectors of Tranqui Island. In contrast, MEKE shows a different seasonal pattern, with relatively higher values in summer than in winter (Figs. 9g–9i). In all three seasons, elevated MEKE values (~0.04 $m^2\ s^{-1}$) are found in the Gulf of Corcovado, south of the Desertores Islands. High values are only observed during summer in the frontal region west of the Comau Fjord and Reñihué Fjord, suggesting enhanced mesoscale variability associated with seasonal frontal dynamics. Overall, the model results indicate that the CIS is characterized by persistent energetic circulation and seasonally enhanced mesoscale variability. This energetic framework provides the background conditions upon which high-frequency processes, such as tidal forcing, may contribute to the generation of strong shear and turbulence.

To assess the role of tidal forcing, the principal semidiurnal constituent (M_2) was isolated from the depth-averaged currents, and its amplitude and associated kinetic energy (KE_{M2}) were computed (Fig. 10). Given the predominantly barotropic nature of the M_2 tide in the study area and its weak seasonal variability, the patterns shown correspond to summer (March) 2023, which is representative of the tidal energy distribution throughout the year. The distribution of the M_2 tidal current amplitude (Fig. 10a) and KE_{M2} (Fig. 10b) reveals multiple energetic hotspots, including the Guafo Mouth, the Chacao Channel, the Desertores Islands, and several channels connecting the open ocean with the Moraleda Channel. These regions coincide with areas of intensified flow identified in Figure 9, suggesting that tidal currents are locally enhanced by bathymetric control and channelized circulation, creating favorable conditions for the generation of strong shear and mixing.

To quantify the relationship between tidal energy and turbulent dissipation, the median dissipation rate (ε) was computed for each station from the vertical profiles obtained during the March, June, and August 2023 field campaigns. These observational estimates were compared with the modeled tidal kinetic energy (KE_{M2}), extracted from the nearest model grid point to each station location (Fig. 10b). The relationship was evaluated in log–log space to better resolve the wide range of variability (Fig. 10c). The results suggest a positive association between KE_{M2} and ε, although with considerable dispersion spanning one to two orders of magnitude for a given tidal energy level. Most observations are concentrated at relatively low KE_{M2} values, where ε exhibits high variability, indicating a strong influence of local processes. At higher KE_{M2} values, ε tends to reach larger magnitudes; however, the limited number of observations in this range prevents the establishment of a robust scaling relationship. A least-square fit in log–log space yields a positive but weak trend, with a sublinear slope (≈ 0.36) and a coefficient of determination $R^2 \approx 0.32$, supporting the idea that tidal energy contributes to turbulence. Overall, these results are consistent with the spatial patterns described above; suggesting that while

https://doi.org/10.5194/egusphere-2026-2889
Preprint. Discussion started: 1 June 2026

tidal forcing provides an important energy source, the magnitude of ε is strongly modulated by local conditions such as stratification, bathymetry, and flow variability.

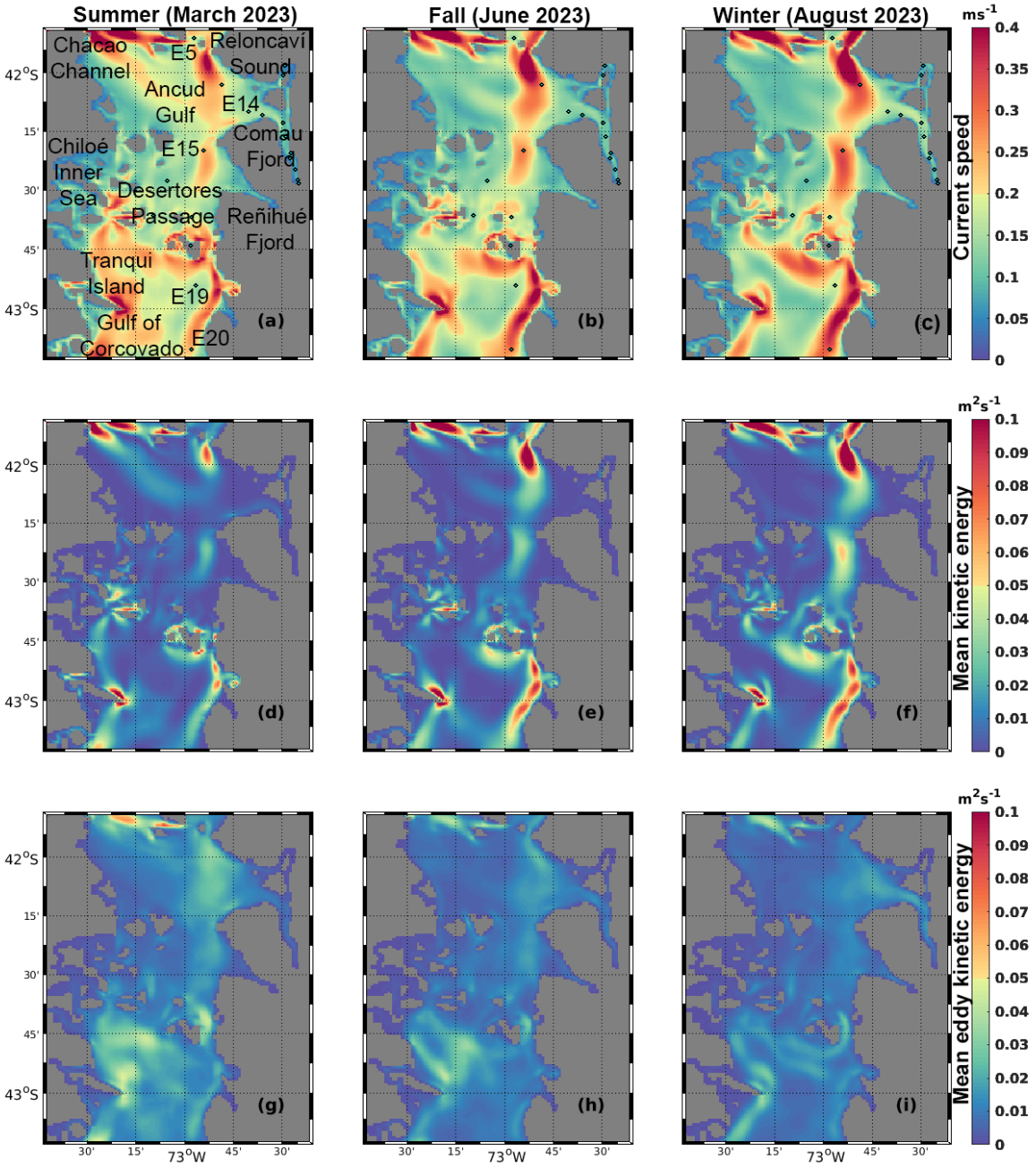

Figure 9. Simulated surface current magnitude from the MOSA model within the Chiloé Inland Sea during (a) summer, (b) autumn, and (c) winter. Mean kinetic energy (MKE) for (d) summer, (e) autumn, and (f) winter. Mean eddy kinetic energy (MEKE) for (g) summer, (h) autumn, and (i) winter.

https://doi.org/10.5194/egusphere-2026-2889
Preprint. Discussion started: 1 June 2026

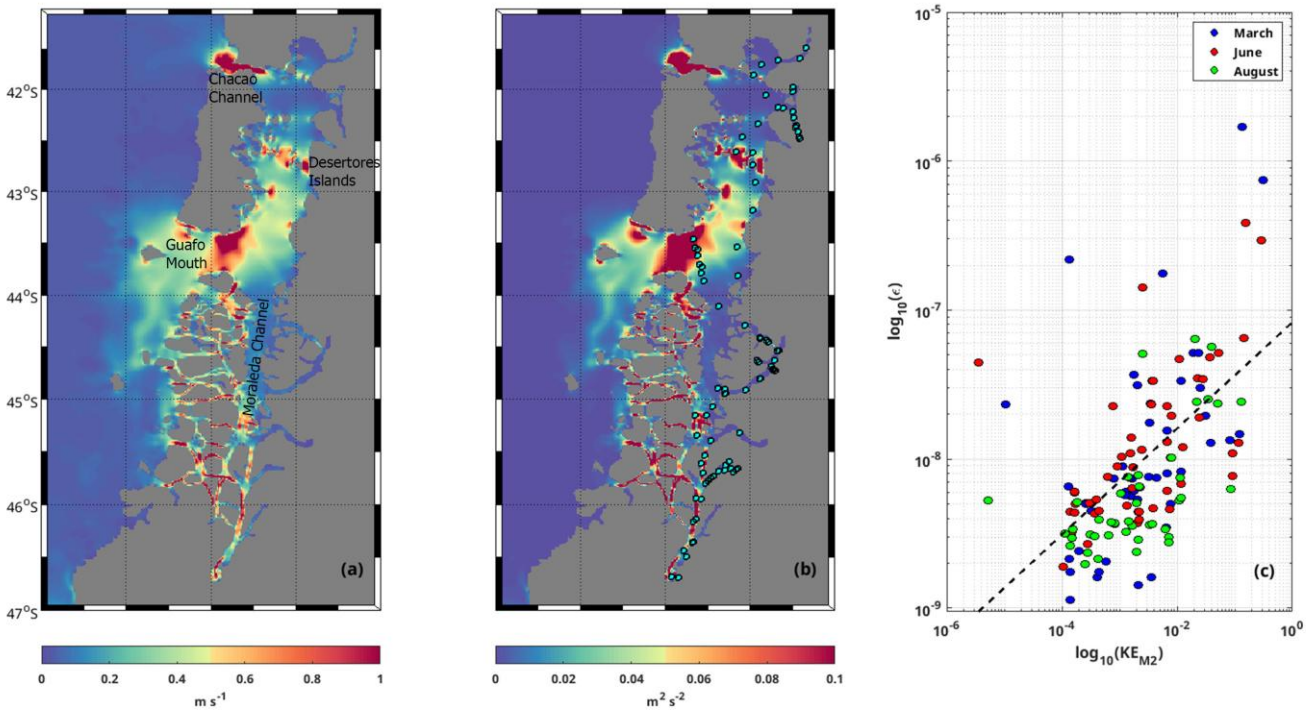

Figure 10. (a) Amplitude of the M_2 tidal current (m s^{-1}) derived from harmonic analysis of depth-averaged model velocities for March 2023. (b) Kinetic energy associated with the M_2 tidal current (KE_{M2}, m^2 s^{-2}), computed from the amplitudes of the zonal and meridional components. (c) Relationship between modeled KE_{M2} and observed turbulent dissipation rates (ε, W kg^{-1}) at station locations for March (blue), June (red), and August (black) 2023. Dissipation values correspond to the median of vertical profiles at each station, and KE_{M2} was interpolated from the model grid. Both axes in (c) are shown in log_{10} scale. The dashed line indicates a least-squares fit in log–log space.

4 Discussion

Previous turbulence measurements in Patagonian fjords revealed intense mixing, particularly near fjord sills and in regions with irregular marine topography (Pérez-Santos et al. 2014; 2018). These findings highlight the important role of turbulence in promoting water column ventilation. However, the impact of turbulence and diapycnal mixing on gas fluxes, such as dissolved oxygen (DO), was not assessed in earlier studies. Addressing this gap is one of the principal motivations for the present manuscript. Seasonal data on hydrographic conditions, vertical shear, and dissolved oxygen were simultaneously collected using a high-resolution (64-512 Hz) turbulence profiler (VMP-250) throughout the fjords and channels of northern Patagonia in 2023. The results revealed intense turbulence in the Chiloé Inner Sea, which facilitated mixing across the entire water column (~200 m depth) and led to events of positive DO fluxes. Conversely, in the Puyuhuapi Fjord, elevated diapycnal mixing was primarily associated with changes in stratification and dense water intrusions, favoring subsurface and deep positive DO fluxes even when local dissipation rates were comparatively lower. These contrasting

https://doi.org/10.5194/egusphere-2026-2889
Preprint. Discussion started: 1 June 2026

behaviors suggest the coexistence of distinct ventilation regimes within the northern Patagonian fjords, motivating the following discussion.

4.1 Water column conditions and turbulence.

The density anomaly distribution along the northern Patagonian fjords showed a clear seasonal correspondence between the less-dense water (10 kg m^{-3}) and the oxygenated water column (90% saturation and 300 μM), in particular near the tidewater glacier of the San Rafael Lagoon. In contrast, dense waters coincided with subsurface and deep hypoxic conditions observed primarily in the Puyuhuapi Fjord. Depending on the season, these dense and low-oxygen waters extended toward the Jacaf Channel and the southern Corcovado Gulf (Fig. 3), reflecting variability in the exchange between oceanic and fjord waters. Hypoxic conditions were reported in the Puyuhuapi Fjord back in the 1970s by the Hudson expedition (Linford et al., 2023), before this area was used extensively for salmon aquaculture (Soto et al., 2004, 2021). Moreover, a significant effort to understand DO distribution in Patagonian fjords was conducted during the 1990s and early 2000s by the CIMAR cruise, supported by the Chilean Navy (Siever and Silva, 2008; Silva, 2008). As one of the main results of this initial effort, the relationship between the presence of low DO and hypoxic water regions and the position of the salty, poorly oxygenated Equatorial Subsurface Water (ESSW) within fjords was identified (Silva, 2008; Silva and Vargas, 2014; Schneider et al., 2014).

Additionally, Linford et al. (2024) demonstrated that not only did the ESSW contribute to hypoxic and low-DO conditions in fjords, but also that these conditions are driven by the dominance of community respiration over gross primary production, especially in the Puyuhuapi Fjord. On the other hand, the Chiloé Inner Sea (e.g., Desertores Island Passage) showed higher values of DO from the surface layer to the bottom (~200 μM) during fall and winter 2023 (Fig. 3e, 3f) associated with lower buoyancy frequency values, evidencing a thoroughly mixed water column (Fig. 4). Ruiz et al. (2021) computed the buoyancy frequency and potential energy anomaly in the northern Patagonian Fjords, identifying the Chiloé Inner Sea as a region of persistent mixing, mainly explained by decreases in river discharge and intensified winds, particularly during fall and winter. In addition to atmospheric and buoyancy forcing, the Chiloé Inner Sea is subject to strong tidal currents and current–topography interactions that enhance vertical shear and sustain mixing throughout the year. In contrast, during summer, thermal stratification dominated, coinciding with the distribution of the 200 μM oxycline shown in Figure 3. However, the decreases in river discharge (Davila et al., 2002; Calvete and Sobarzo, 2011) and wind intensification (Pérez-Santos et al., 2019; Soto-Riquelme et al., 2023) affect the entire northern Patagonian fjords systems during fall and winter, with mixing conditions varying spatially and a majority of sheltered inner fjords remaining relatively stratified (Fig. 4). This spatial heterogeneity reflects differences in residence time and geometric confinement, as freshwater can remain trapped inside fjords for extended periods, often exceeding 100 days (Linford et al., 2024), thereby maintaining vertical stability despite seasonal atmospheric forcing. Lueck et al. (2013) proposed that in unsteady flow, the production and dissipation of turbulent kinetic energy are nearly equal. In contrast, under stable conditions, approximately 20% of the energy produced increases the fluid's potential energy, while the remaining 80% is dissipated as turbulent kinetic energy.

https://doi.org/10.5194/egusphere-2026-2889
Preprint. Discussion started: 1 June 2026

As a result of this study, in-situ turbulence measurements in the northern Patagonian fjords revealed, for the first time, intense dissipation rates of turbulent kinetic energy ($\varepsilon=5\times10^{-10}$ W kg^{-1}) in the Chiloé Inner Sea (Fig. 5 , Fig. 7). This elevated dissipation is identified as a key mechanism sustaining the persistent mixing conditions discussed previously and reported by Ruiz et al. (2021), based on data from the oceanographic and operational MOSA numerical model. In addition, other small areas exhibiting intense dissipation, such as Paso Queullín and the region between Quitralco Fjord and San Rafael Lagoon, were also identified. These zones displayed higher diapycnal eddy diffusivity values, approximately 10^{-3} m^2 s^{-1} (Fig. 5), indicating enhanced vertical exchange across density gradients. Abrupt topographic changes (Fig. 1) and the interaction of barotropic currents, modulated by semidiurnal tides with islands, passages, and channels appear to be primary drivers of the intense turbulence in the Chiloé Inner Sea (Fig. 9, Fig. 10). The dominance of semidiurnal tidal currents in this region has been documented by Artal et al. (2019), supporting the role of tidal forcing in sustaining shear-driven mixing. Pérez-Santos et al. (2018) similarly observed intense turbulent mixing around a shallow sill at the confluence of the Puyuhuapi Fjord and the Jacaf Channel. The dissipation rates of turbulent kinetic energy and diapycnal eddy diffusivity reported by Pérez-Santos et al. (2018) were comparable to those recorded in this study. As a result, this turbulence contributed to the aggregation of zooplankton and fish by enhancing nutrient injection into the photic layer, highlighting the significance of intense turbulence in biogeochemical and biological cycles (Klymak and Gregg, 2004; Whitney et al., 2014). Beyond the regions dominated by turbulence and high diapycnal eddy diffusivity, elevated values of this variable were also observed in the subsurface layers of other areas. Notable examples are the Aysén, Puyuhuapi, and Comau fjords (Figures 5d–f), where buoyancy frequency likely modulates vertical mixing intensity. Together, these results indicate that spatial contrasts in stratification, tidal forcing, and residence time jointly regulate oxygen renewal and vertical exchange processes across the northern Patagonian fjords.

4.2 Mechanisms involved in the origin of oxygen fluxes.

The global decline in dissolved oxygen (DO) has become a major concern for the scientific community due to its impacts on marine habitat quality and distribution, biodiversity loss, disease prevalence, greenhouse gas production, and primary production (Bopp et al., 2013; Breitburg et al., 2018a, 2018b; Bhuiyan et al., 2024). Consequently, recent scientific efforts have increasingly focused on identifying the mechanisms and drivers contributing to water ventilation. This process helps balance the loss of oxygen and, in some cases, increases oxygen concentrations in subsurface and deep oceanic waters (Fig. 6). In this context, we evaluate the role of mechanical turbulence and diapycnal mixing in enhancing DO concentrations by quantifying DO fluxes using a VMP-250 microstructure profiler in selected areas of the northern Patagonian fjords. These regions have historically exhibited hypoxic and low-oxygen conditions, as reported in previous studies (Sievers and Silva, 2008; Silva and Vargas, 2014; Schneider et al., 2014; Linford et al., 2024). The results showed a significant number of positive DO flux events in the Chiloé Inner Sea during summer and fall 2023, primarily explained by

https://doi.org/10.5194/egusphere-2026-2889
Preprint. Discussion started: 1 June 2026

intense turbulent mixing generated by the interaction of the semidiurnal tide with local topography, constituting the first identified mechanism responsible for positive DO flux events in the northern Patagonian fjords. Numerical model results indicated strong meridional currents at stations where enhanced shear layers were detected, particularly when the flow crossed the Desertores Islands (Fig. 8). Intense zonal currents driven by passage and channel constrictions increased mean kinetic and eddy kinetic energy (Fig. 9), thereby promoting turbulent energy dissipation in this area.

Furthermore, the numerical model highlighted the significance of the M_2 harmonic (Fig. 10) as a principal tidal constituent influencing the circulation variability (Fig. 9), consistent with a previous barotropic tidal simulation of the Chiloé Inner Sea (Aiken, 2008), and subsequent analyses of semidiurnal tidal variability in the region (Artal et al., 2019). The model results indicate that the M_2 constituent plays a significant role in the tidal dynamics of the system, with differences in amplitude, phase, and propagation of tidal constituents between the northern and southern Chiloé Inner Sea. Aiken, (2008) showed that a resonance frequency close to the semidiurnal tide contributed to a higher amplitude of semidiurnal constituents north of the Desertores Islands. In contrast, in the southern region, resonance was not observed due to numerous channels and passages that facilitate the exchange of Pacific Ocean water with the fjord system. This mechanism is further supported by recent modeling of subtidal transport through the Guafo Mouth, demonstrating that semidiurnal tidal forcing modulates ocean–fjord exchange and associated property fluxes (Mundaca et al., 2025). Ross et al. (2025) utilized in-situ data from an oceanographic mooring equipped with an Acoustic Doppler Current Profiler (ADCP) at the Guafo mouth to demonstrate that subtidal processes are the primary drivers of exchange between the northern Patagonian fjords and the adjacent Pacific Ocean. Additionally, high-frequency observations in Reloncaví Sound reveal pronounced diurnal–semidiurnal shear and mixing linked to tidal dynamics, reinforcing the role of semidiurnal variability in structuring physical and biogeochemical processes within the inner sea (Pérez-Santos et al., 2025). These findings are consistent with the results presented here, where tidal energy contributes to turbulent dissipation, although its effect is strongly modulated by local conditions.

The advection of dense water into the Puyuhuapi Fjord (Fig. 3a) leads to changes in subsurface and deep buoyancy, enhancing vertical density gradients and promoting intense diapycnal eddy diffusivity (Fig. 5d). This process generates positive DO flux events (Fig. 6a) and, consequently, reduces hypoxic conditions in the area (Fig. 3d), thereby constituting the second mechanism involved in the origin of these events. For instance, Pinilla et al. (2020) reported a deep-water renewal in the Puyuhuapi Fjord associated with increased inflow of dense water, which favors the formation of deep-oxygenated waters. Additionally, Linford et al. (2023) and Ross et al. (2025) reported the significance of the oceanic-fjord interchange through the Guafo Mouth, particularly the contribution of the oxygenated SAAW to ventilation and its distribution within the Patagonian fjord system. Such renewal events represent a key ventilation mechanism that enhances deep oxygen concentrations and improves overall water quality in fjord systems. Accordingly, deep-water renewals have long been recognized as a fundamental process in fjord biogeochemistry, from early observations (Anderson and Devol, 1973) to recent assessments (Salvanes et al., 2025).

https://doi.org/10.5194/egusphere-2026-2889
Preprint. Discussion started: 1 June 2026

Finally, double-diffusive convection (DDC), as measured by the Turner angle, may represent an additional mechanism favoring positive DO flux in Patagonian fjords, particularly under stratification regimes established by dense-water intrusions and subsequent vertical density gradients. Analysis of the dataset collected in this study indicates a predominance of diffusive-layering over salt-fingering events (Figures A1 and A2 in the Appendix), with a substantial number of medium- and strong-intensity diffusive-layering episodes identified in the study area, consistent with observations by Pérez-Santos et al. (2014) in another Patagonian fjord. These conditions suggest that DDC may enhance vertical redistribution of dissolved oxygen across stratified interfaces, potentially acting in concert with tidal mixing and deep-water renewal processes described above. However, the specific quantitative contribution of DDC on positive DO flux remains uncertain and warrants further investigation in future studies.

5 Conclusions

Hydrographic, turbulence, and dissolved oxygen data were collected using a vertical microstructure profiler in the northern Patagonian fjords and channels to evaluate, for the first time, whether positive dissolved oxygen fluxes contribute to deep-water ventilation in areas where poorly oxygenated and hypoxic waters have been observed. Measurements revealed dense water in the Puyuhuapi Fjord and the Jacaf Channel, coinciding with regions of hypoxia. Furthermore, the extent of hypoxic areas varied throughout the year under investigation (2023), with a marked reduction during the summer. Diapycnal mixing was identified as a key process promoting positive dissolved oxygen fluxes in the subsurface layer of the Puyuhuapi Fjord in summer (March) 2023. This process was facilitated by the advection of dense oceanic water into the fjord, thereby reducing hypoxic conditions. In contrast, intense turbulence detected in the Chiloé Inner Sea was a major mechanism associated with positive dissolved oxygen flux events across the seasons, linked to the interaction of semidiurnal tidal currents with local topography. Together, these findings indicate that oxygen ventilation in northern Patagonian fjords is governed by the interplay between barotropic tidal forcing, deep-water renewal, and stratification-controlled mixing processes. The present study demonstrates the importance of utilizing a single instrument to evaluate the effects of mechanical turbulence and diapycnal mixing on key gas fluxes (e.g., dissolved oxygen) that are crucial for sustaining marine biodiversity and habitats, as well as for understanding the dynamics of globally distributed hypoxic areas. These results contribute to a mechanistic understanding of how regional hydrodynamics regulate oxygen redistribution in semi-enclosed coastal environments, which is essential for anticipating the response of fjord ecosystems to ongoing ocean deoxygenation driven by climate change.

https://doi.org/10.5194/egusphere-2026-2889
Preprint. Discussion started: 1 June 2026

APENDIX A

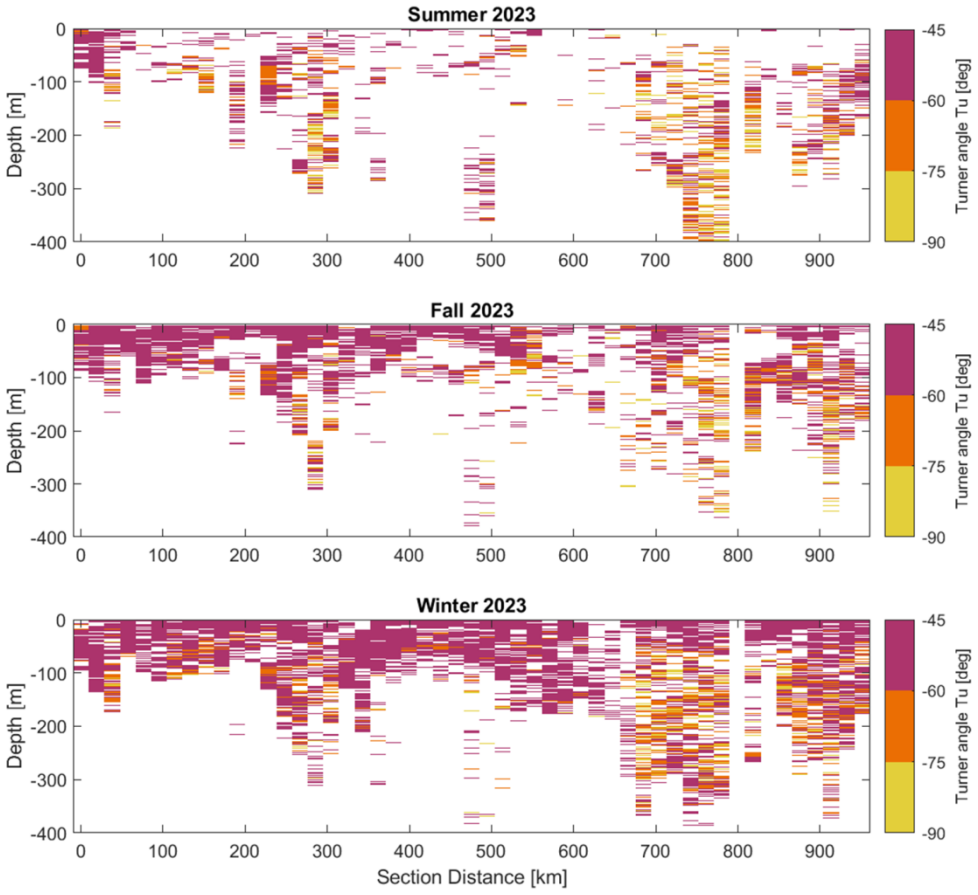

Figure A1. Turner angle (Tu) calculation using the methodology proposed by You (2002), along a vertical section in the northern Patagonian fjords during 2023. Results represented only the diffusive-layering events, divided into strong (Tu between –90° and -75°), medium (Tu between -75° and -60°), and weak (Tu between -60° and -45°).

https://doi.org/10.5194/egusphere-2026-2889
Preprint. Discussion started: 1 June 2026

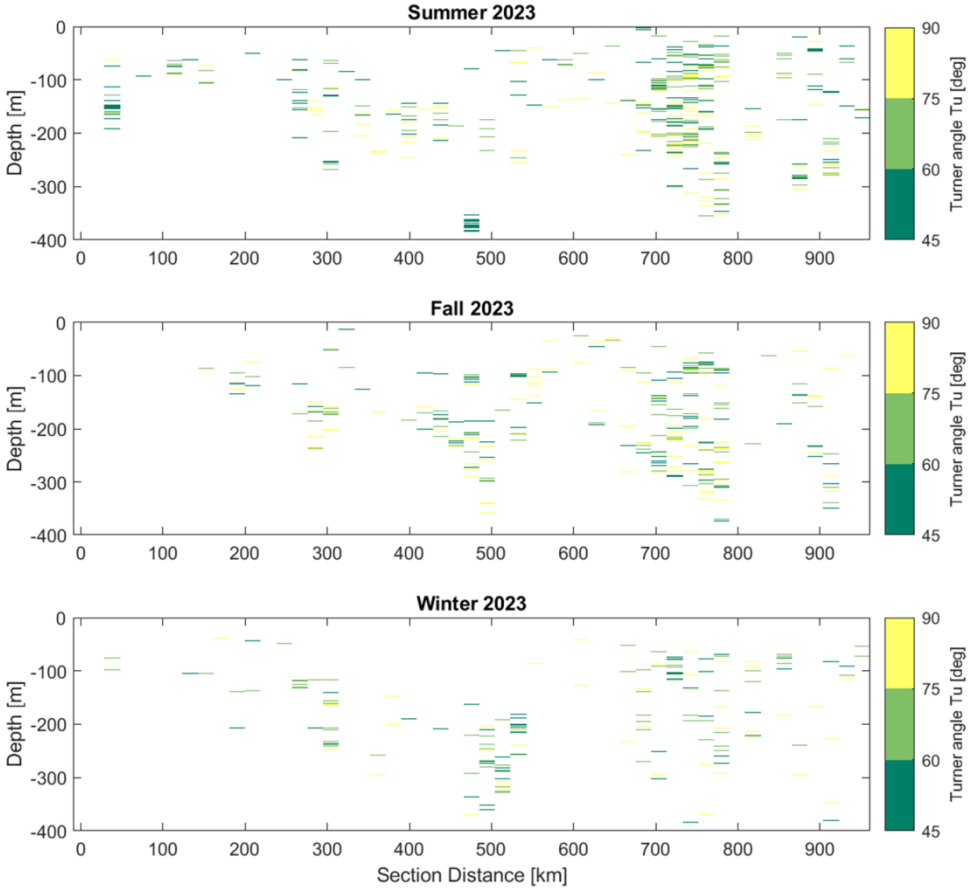

Figure A2. Turner angle (Tu) calculation using the methodology proposed by You (2002), along a vertical section in the northern Patagonian fjords during 2023. Results represented only the salt fingering events (Tu between 90° and 45°).

Conflict of Interest

The authors declare no conflicts of interest relevant to this study.

https://doi.org/10.5194/egusphere-2026-2889
Preprint. Discussion started: 1 June 2026

Author Contributions

IPS: led study design, collection and analysis of physical oceanographic, and manuscript leader. PL, LR, MR: analysis of turbulence data, and manuscript revision. OA, EP: development and analysis of numerical model, and manuscript revision. LR, PD, IM: manuscript revision. GM, GS: data collection. All authors contributed to the writing of the present manuscript.

Funding

Iván Pérez-Santos was funded by FONDECYT 1211037, 1251038, COPAS COASTAL FB210021, and IFOP ID 1049-48-LP22. Lauren Ross acknowledges funding for NSF Grant Number 2045866 that aided in her participation of this study.

Acknowledgments

We thank the crew of the Jürgen Winter for their invaluable support during data collection. Special thanks are extended to the students and technicians for facilitating the collection of turbulence data and ensuring the safe return of the microprofiler.

Competition interests

The authors declare no competing interests.

Data availability statement

Data and metadata are available in Pérez-Santos, I. (2026). Data and metadata from manuscript, Vertical Fluxes of Dissolved Oxygen Driven by Turbulence and Diapycnal Mixing in Patagonian Fjords [Data set]. Zenodo. https://doi.org/10.5281/zenodo.20285180

Reference

Aiken, C. M. (2008). Barotropic tides of the Chilean Inland Sea and their sensitivity to basin geometry. *Journal of Geophysical Research: Oceans*, *113*(C8).

Aiken, C.M., 2012. Seasonal thermal structure and exchange in Baker Channel, Chile. Dynamics of Atmospheres and Oceans 58, 1–19.

Aksnes, D., Elin D., and Jarle B.: Mitigation of oxygen decline in fjords by freshwater injection. Estuarine, Coastal and Shelf Science, Volume 284, 2023, 108286, ISSN 0272-7714, https://doi.org/10.1016/j.ecss.2023.108286, 2023.

Anderson, J., and Devol, A.: Deep water renewal in Saanich Inlet, an intermittently anoxic basin, Estuarine and Coastal Marine Science, Volume 1, Issue 1, Pages 1-10, ISSN 0302-3524, https://doi.org/10.1016/0302-3524 (73)90052-2, 1973.

Artal, O., Pizarro, O., & Sepúlveda, H. H. (2019). The impact of spring-neap tidal-stream cycles in tidal energy assessments in the Chilean Inland Sea. *Renewable Energy*, *139*, 496-506.

Botes, M., Kwaadsteniet M., and Cloete, T.: Application of quantitative PCR for the detection of microorganisms in water. Analytical and Bioanalytical Chemistry 405, 91-108, 2013.

https://doi.org/10.5194/egusphere-2026-2889
Preprint. Discussion started: 1 June 2026

Breitburg, D., Grégoire, M. and Isensee, K.: Global Ocean Oxygen Network. The ocean is losing its breath: Declining oxygen in the world's ocean and coastal waters' IOC-UNESCO, IOC Technical Series, No. 137 40pp, 2018a.

Breitburg, D. et al.: Declining oxygen in the global ocean and coastal waters. Science 359, 1-11, 2018b.

Bhuiyan, Md., Rahman, M., Naher, S., Shahed, Z., Mohammad, A., Islam, A.: Oxygen declination in the coastal ocean over the twenty-first century: Driving forces, trends, and impacts, Case Studies in Chemical and Environmental Engineering, Volume 9, 100621, ISSN 2666-0164, https://doi.org/10.1016/j.cscee.2024.100621, 2024.

Dávila, P.M., Figueroa, D., and Müller, E.: Freshwater input into the coastal ocean and its relation with the salinity distribution off austral Chile (35–55_S). Continental Shelf Research 22–3, 521–534, 2002.

Calvete, C., Sobarzo, M.: Quantification of the surface brackish water layer and frontal zones in southern Chile an fjords between Boca del Guafo (43_300S) and Estero Elefantes (46_300S). Continental Shelf Research 3, 162–171, 2011.

Conley, D.J., Carstensen, J., Vaquer-Sunyer, R. et al.: Ecosystem thresholds with hypoxia. Hydrobiologia 629, 21–29, https://doi.org/10.1007/s10750-009-9764-2, 2009.

Cuypers, Y., Bouruet-Aubertot, P., Marec, C. Fuda, J.-L.: Characterization of turbulence and validation of fine-scale parametrization in the Mediterranean Sea during BOUM experiment, Biogeosciences Discuss., 8, 8961–8998, doi:10.5194/bgd-8-8961-2011, 2011.

Debreu, L., Marchesiello, P., Penven, P., & Cambon, G. (2012). Two-way nesting in split-explicit ocean models: Algorithms, implementation and validation. *Ocean Modelling*, *49*, 1-21.

Drevillon, M., Bourdalle-Badie, R., Derval, C., Lellouche, J. M., Rémy, E., Tranchant, B., ... & Parent, L. (2008). The GODAE/Mercator-Ocean global ocean forecasting system: results, applications and prospects. *Journal of Operational Oceanography*, *1*(1), 51-57.

Egbert, G. D., & Erofeeva, S. Y. (2002). Efficient inverse modeling of barotropic ocean tides. *Journal of Atmospheric and Oceanic technology*, *19*(2), 183-204.

Holtermann, P., Pinner, O., Schwefel, R., and Umlauf, L.: The role of boundary mixing for diapycnal oxygen fluxes in a stratified marine system. Geophysical Research Letters, 49, e2022GL098917. https://doi.org/10.1029/2022GL098917, 2022.

Osborn, T. R.: Estimates of the local rate of vertical diffusion from dissipation measurements, J. Phys. Oceanogr., 10, 83–89, 1980.

Jackson, J. M., Bianucci, L., Hannah, C. G., Carmack, E. C., and Barrette, J.: Deep waters in British Columbia mainland fjords show rapid warming and deoxygenation from 1951 to 2020. Geophysical Research Letters, 48 (3), e2020GL091094. https://doi.org/10.1029/2020GL091094, 2021.

Klymak, J. M. and Gregg, M. C.: Tidally Generated Turbulence over the Knight Inlet Sill, American Meteorological Society, https://doi.org/10.1175/1520-0485(2004)034<1135:TGTOTK>2.0.CO;2, 1–17, 2004.

Levin, L.A.: Manifestation, Drivers, and Emergence of Open Ocean Deoxygenation. Annual Review of Marine Science, 10, 229-260. https://doi.org/10.1146/annurev-marine-121916-063359, 2018.

https://doi.org/10.5194/egusphere-2026-2889
Preprint. Discussion started: 1 June 2026

Linford, P., Pérez-Santos, I., Montes, I., Dewitte, B., Buchan, S., Narváez, D., et al.: Recent deoxygenation of Patagonian fjord subsurface waters connected to the Peru–Chile undercurrent and equatorial subsurface water variability. Global Biogeochemical Cycles, 37, e2022GB007688. https://doi. org/10.1029/2022GB007688, 2023.

Linford, P., Pérez-Santos, I., Montero, P., et al.: Oceanographic Processes Driving Low Oxygen Conditions Inside Patagonian Fjords. Biogeosciences, 21, 1433–1459, https://doi.org/10.5194/bg-21-1433-2024, 2024.

Lozovatsky, I., Escauriaza, C., Suarez, L. et al.: A snapshot of turbulence in the Northeastern Magellan Strait. Ocean Dynamics 74, 459–469, https://doi.org/10.1007/s10236-024-01613-y, 2024.

Luketina, D.A., Imberger, J.: Determining turbulent kinetic energy dissipation from Bachelor curve fitting. Journal of Atmospheric and Oceanic Technology 18, 100–113. http://dx.doi.org/10.1175/1520-0426, 2001.

Moreno-Meynard, P., Artal, O., Torres, R., & Reid, B. (2024). Flow-weighted sourcing of freshwater runoff from Pacific-draining continental and coastal basins in south-western Patagonia (41-56° S): characterizing regional inputs to Chilean fjords. *Frontiers in Marine Science*, *11*, 1396570.

Mundaca, V., Echevin, V., Vergara, O. A., Artal, O., & Sepúlveda, H. H. (2025). Dynamics of the subtidal transport through the Guafo Mouth connecting the open ocean and the Chilean Inland Sea in southern Chile. *Continental Shelf Research*, *288*, 105428.

Pawlowicz, R., Beardsley, B., & Lentz, S. (2002). Classical tidal harmonic analysis including error estimates in MATLAB using T_TIDE. *Computers & geosciences*, *28*(8), 929-937.

Penven, P., Debreu, L., Marchesiello, P., & McWilliams, J. C. (2006). Evaluation and application of the ROMS 1-way embedding procedure to the central California upwelling system. *Ocean Modelling*, *12*(1-2), 157-187.

Pérez-Santos, I., Garcés-Vargas, J., Schneider, W., Ross, L., Parra, S., and Valle-Levinson, A.: Double-diffusive layering and mixing in Patagonian fjords, Prog. Oceanogr., 129, 35–49, https://doi.org/10.1016/j.pocean.2014.03.012, 2014.

Pérez-Santos, I., Castro, L., Ross, L., Niklitschek, E., Mayorga, N., Cubillos, L., Gutierrez, M., Escalona, E., Castillo, M., Alegría, N., and Daneri, G.: Turbulence and hypoxia contribute to dense biological scattering layers in a Patagonian fjord system, Ocean Sci., 14, 1185–1206, https://doi.org/10.5194/os-14-1185-2018, 2018.

Pérez-Santos, I., Díaz, P., Silva, N., et al.: Oceanography time series reveals annual asynchrony input between oceanic and estuarine waters in Patagonian fjords, Sci. Total Environ., 798, 149241, https://doi.org/10.1016/j.scitotenv.2021.149241, 2021.

Pérez-Santos, I., Díaz, P. A., Ross, L., Riquelme-Bugueño, R., Lara, C., Barrera, F., ... & Saldías, G. S. (2025). On the diurnal-semidiurnal cycles of physical and biological inter-processes in the upper water column of Reloncaví Sound, northern Patagonia. *Marine Environmental Research*, 107482.

Pinilla, E., Castillo, M. I., Pérez-Santos, I., Venegas, O., and Valle-Levinson, A.: Water age variability in a Patagonian fjord, J. Mar. Syst., 210, 103376, https://doi.org/10.1016/j.jmarsys.2020.103376, 2020.

https://doi.org/10.5194/egusphere-2026-2889
Preprint. Discussion started: 1 June 2026

Ross, L., Pérez-Santos, I., Linford, P., Díaz, P.: Circulation in the Guafo Mouth: The gateway to northern Patagonia, Science of The Total Environment, Volume 979, 179512, ISSN 0048-9697, https://doi.org/10.1016/j.scitotenv.2025.179512, 2025.

Ruddick, B., Anis, A., Thompson, K.: Maximum likelihood spectral fitting: the Bachelor spectrum. Journal of Atmospheric and Oceanic Technology 17, 1541–1555. http://dx.doi.org/10.1175/1520-0426, 2000.

Ruiz, C., Artal, O., Pinilla, E., and Sepúlveda, H. H.: Stratification and mixing in the Chilean Inland Sea using an operational model, Ocean Modell., 158, 101750, https://doi.org/10.1016/j.ocemod.2020.101750, 2021.

Salvanes, A.G.V., Gallo, N.D., Solås, M.R., Saltalamacchia, F., Aksnes, D.L., Darelius, E., Christiansen, S., Folkvord, A., Hosia, A., Kaartvedt, S., Levin, L., Limburg, K., Martell, L., Midtøy, F., Myksvoll, M., Risebrobakken, B., Savolainen, H., Skadal, J. and Staby, A.: Deep Fjords Are Excellent Natural Infrastructure for Climate Impact Studies. Fish Fish, 26: 270-277. https://doi.org/10.1111/faf.12879, 2025.

Silva, N. and Vargas, C.: Hypoxia in Chilean Patagonia fjords, Progress in Oceanography, Vol. 129, 62-74, 2014.

Sievers, A.H. and Silva, N.: Water masses and circulation in austral Chilean channels and fjords, in: Silva, N., Palma, S. (Eds.), Progress in the oceanographic knowledge of Chilean inner waters, from Puerto Montt to Cape Horn. Comité Oceanográfico Nacional - Pontificia Universidad Católica de Valparaíso, Valparaíso, Chile, pp. 53-58. Book on line at http://www.cona.cl/, 2018.

Silva, N. and Vargas, C. (2014). Hypoxia in Chilean Patagonia fjords, Progress in Oceanography, Vol. 129, 62-74.

Skamarock, W. C., & Klemp, J. B. (2008). A time-split nonhydrostatic atmospheric model for weather research and forecasting applications. *Journal of computational physics*, *227*(7), 3465-3485.

Solås, M. R., Anne G. S., and Dag L. A.: Association between water darkening and hypoxia in a Norwegian fjord, Estuarine, Coastal and Shelf Science, Volume 310, 2024, 108988, ISSN 0272-7714, https://doi.org/10.1016/j.ecss.2024.108988.

Soto, D. and Norambuena, F.: Evaluation of salmon farming effects on marine systems in the inner seas of southern Chile: a large scale mensurative experiment, J. Appl. Ichthyol., 20, 493–501, https://doi.org/10.1111/j.1439-0426.2004.00602, 2004.

Soto, D., León-Muñoz, J., Garreaud, R., Quiñones, R. A., and Morey, F.: Scientific warnings could help to reduce farmed salmon mortality due to harmful algal blooms, Mar. Pol., 132, 104705, https://doi.org/10.1016/j.marpol.2021.104705, 2021.

Soto-Riquelme, C., Pinilla, E., and Ross, L.: Wind influence on residual circulation in Patagonian channels and fjords,Continental Shelf Research,Volume 254, 104905, ISSN 0278-4343, https://doi.org/10.1016/j.csr.2022.104905, 2023,

Schmidtko, S., Stramma, L., and Visbeck, M.: Decline in global oceanic oxygen content during the past five decades, Nature, 542, 335–339, https://doi.org/10.1038/nature21399, 2017.

https://doi.org/10.5194/egusphere-2026-2889
Preprint. Discussion started: 1 June 2026

635 Schneider, W., Pérez-Santos, I., Ross, L., Bravo, L., Seguel, R., and Hernández, F.: On the hydrography of Puyuhuapi
636 Channel, Chilean Patagonia, Prog. Oceanogr., 129, 8–18, https://doi.org/10.1016/j.pocean.2014.03.007, 2014.
637 Shih, L. H., Koseff, J. R., Ivey, G. N., Ferziger, J.: Parameterization of turbulent fluxes and scales using homogeneous
638 sheared stably stratified turbulence simulations, J. Fluid Mech., 525, 193–214, 2005.
639 Steinbuck, J.V., Mark, T.S., Stephen, G.M.: An evaluation of χT estimation techniques: Implications for Bachelor fitting and
640 e. Journal of Atmospheric and Oceanic Technology 26, 1652–1662, 2009.
641 Thorpe, S. A. (2005). The turbulence ocean. Cambridge University Press, CB2 2RU, UK, 426 pp.
642 Whitney, M., Jia, Y., McManus, P. M., and Kunz, C. J.: Sill effects on physical dynamics in eastern Long Island Sound,
643 Ocean Dynam., 64, 443–458, https://doi.org/10.1007/s10236-013-0681-6, 2014.
644 You, Y.: A global ocean climatological atlas of the Turner angle: implications for double-diffusion and water-mass structure.
645 Deep-Sea Research I 49, 2075–2093, 2002.
646